CP violation and the fourth generation

Gad Eilam,[1,*] Blaženka Melić,[2,†] and Josip Trampetić[3,‡]

[1]*Department of Physics, Technion, Israel Institute of Technology, Haifa, 32000, Israel*
[2]*Theoretical Physics Division, Rudjer Bošković Institute, Bijenička 54, HR -10002 Zagreb, Croatia*
[3]*Rudjer Bošković Institute, Bijenička 54, HR-10002 Zagreb, Croatia*
(Received 12 October 2009; published 21 December 2009)

Within the standard model with the 4th generation quarks b' and t' we have analyzed *CP*-violating flavor changing neutral current processes $t \to cX$, $b' \to sX$, $b' \to bX$, $t' \to cX$, and $t' \to tX$, with $X = H, Z, \gamma, g$, by constructing and employing a global, unique fit for the 4th generation mass mixing matrix (CKM4) at $300 \le m_{t'} \le 700$ GeV. All quantities appearing in the CKM4 were subject to our fitting procedure. We have found that our fit produces the following *CP* partial rate asymmetry dominance: $a_{CP}(b' \to s(H, Z; \gamma, g)) \simeq (94, 62; 47, 41)\%$, at $m_{t'} \simeq 300, 350$ GeV, respectively. From the experimental point of view the best decay mode, out of the above four, is certainly $b' \to s\gamma$, due to the presence of the high energy single photon in the final state. We have also obtained relatively large asymmetry $a_{CP}(t \to cg) \simeq (8 - 18)\%$ for t' running in the loops. There are fair chances that the 4th generation quarks will be discovered at LHC and that some of their decay rates will be measured. If b' and t' exist at energies we assumed, with well executed tagging, large a_{CP} could be found too.

DOI: 10.1103/PhysRevD.80.116003 PACS numbers: 11.30.Er, 11.30.Hv, 12.60.−i

I. INTRODUCTION

In this paper the main idea is to find possibly large genuine *CP* violation (CPV) effects in the decays of the fourth generation of quarks, arising from the one-loop flavor changing neutral currents (FCNC), by using unique fitting procedure.

A fourth generation of quarks and leptons, which we refer to as (t', b', ℓ', ν'), in our opinion is one of the most conservative guesses one could make as to what new physics lies ahead. Since the 4th generation of flavors is neither predicted nor disallowed by the standard model (SM3) we should keep an open mind regarding its existence.

Since possible existence of the 4th generation provides a number of desirable features, for a review see [1] and for a more updated review see [2], let us first remind the reader of those.

(i) Fourth family is consistent with electroweak (EW) precision tests [3], because, if the 4th generation of fermions satisfy the following constraint for quarks [4],

$$m_{t'} - m_{b'} \simeq \left(1 + \frac{1}{5}\ln\frac{m_H}{115\text{ GeV}}\right) \times 55\text{ GeV}, \quad (1.1)$$

and the related 4th lepton generation mass difference $m_{l'} - m_{\nu'} \simeq 60$ GeV [4], the electroweak oblique parameters [5] are not extending the experimentally allowed parameter space.

(ii) The 4th family of fermions is consistent with SU(5) gauge coupling, i.e., it can be unified without supersymmetry, and, because of (1.1), the 4th generation softens the current Higgs bounds [6].

(iii) With respect to quark-neutrino physics, if the 4th generation were discovered, it may change our prediction for the $K^+ \to \pi^+ \nu\bar{\nu}$ decay [7]. There can also be implications on other penguin-induced decays, like $b \to s\gamma$ and $b \to s\phi$; see [8,9], respectively.

(iv) A heavy 4th family could naturally play a role in the dynamical breaking of EW symmetry [10,11].

(v) If the unitarity of SM3 CKM matrix $V_{3\times3} = V_{\text{CKM3}}$ is slightly broken, new information from top-quark production at Tevatron still leaves open the possibility that $|V_{tb}|$ is nontrivially smaller than 1 [12].

(vi) In addition, a new generation might also cure some flavor physics problems too [10,13].

(vii) Finally, the 4th family might solve baryogenesis related problems, by visible increase of the measure of *CP* violation and the strength of the phase transition. Namely, the question of the large *CP* violation in the SM3 extended to the 4th generation of fermions (SM4) was recently raised in [14], with respect to the insufficient *CP* asymmetry produced in the standard model with three generation for generating the baryon asymmetry in the universe.

There is a known quantity, the Jarlskog invariant, which measures the *CP* violation in the model. For SM3, it is defined as [15]

$$J = (m_t^2 - m_u^2)(m_t^2 - m_c^2)(m_c^2 - m_u^2)(m_b^2 - m_d^2)(m_b^2 - m_s^2) \times (m_s^2 - m_d^2)A, \quad (1.2)$$

*eilam@physics.technion.ac.il
†melic@thphys.irb.hr
‡josipt@rex.irb.hr

where A is twice of the area of any of six unitary triangles in SM3 and it is of the order of $O(10^{-5})$.

The fourth generation is added to the three known $SU(2)_f$ doublets as

$$\begin{pmatrix} t' \\ b' \end{pmatrix}. \tag{1.3}$$

So in the case of SM4, the above relation (1.2) in the $d - s$ degeneracy limit generalizes to [14]

$$J_{234}^{bs} = (m_{t'}^2 - m_c^2)(m_{t'}^2 - m_t^2)(m_t^2 - m_c^2)(m_{b'}^2 - m_s^2) \times (m_{b'}^2 - m_b^2)(m_b^2 - m_s^2)A_{234}^{bs}, \tag{1.4}$$

which, due to the large $m_{b'}$, $m_{t'}$ masses and somewhat larger area of the $b \to s$ quadrangle A_{234}^{bs} corresponding to the SM4 unitarity relation $V_{4\times4}V_{4\times4}^{\dagger} = 1$, can be up to 15 orders of magnitude larger than the Jarlskog invariant in the SM3 [14]. However, this enhancement of CPV in the model with 4th fermion generation cannot, by itself, solve the problem of the baryogenesis, since just adding the fermions reduces the electroweak phase transition if there are not some additional theories involved like supersymmetry [16], or the theory with at least two Higgs doublets [17].

We start our analysis by performing a fit of SM4 CKM mass matrix. To obtain valid CPV results it is also crucial to follow results of the general fit of the electroweak precision data, since, in order to be able to calculate the real value of A_{234}^{bs}, it is necessary to make a global fit of a complete $V_{4\times4}$ matrix. Therefore, on top of many different processes used in the fit, we have also taken into account the EW constraints on the CKM mixing between the 3rd and the 4th quark family.

We than compute FCNC processes of the fourth generation quarks, like $b' \to s(H, Z, \gamma, g)$, etc., and analyze the most important consequence: large CP violation in such decays. The rare top decays $t \to c(H, Z, \gamma, g)$, involving the 4th generation quarks running in the loops, are considered too.

The paper is organized as follows. In Sec. II we introduce the quark mixing matrix with 4th generation and construct the fitting procedure, the fit itself, and present the corresponding results, respectively. Section III contains computations of the FCNC processes involving 4th family, while the CP-violation effects due to the 4th generation are discussed in Sec. IV. Lastly, Sec. V is devoted to discussions and a conclusion.

II. CKM MATRIX FOR THE FOURTH GENERATION

The fourth generation 4×4 quark mixing matrix is given by

$$V_{4\times4} \equiv V_{\mathrm{CKM4}} = \begin{pmatrix} V_{ud} & V_{us} & V_{ub} & V_{ub'} \\ V_{cd} & V_{cs} & V_{cb} & V_{cb'} \\ V_{td} & V_{ts} & V_{tb} & V_{tb'} \\ V_{t'd} & V_{t's} & V_{t'b} & V_{t'b'} \end{pmatrix}. \tag{2.1}$$

The parametrization of such a matrix can be done in many possible ways. We have chosen to use the standard CKM3 Wolfenstein parametrization [18] of the 3×3 matrix, up to $O(\lambda^5)$

$$V_{\mathrm{CKM3}} = \begin{pmatrix} V_{ud} & V_{us} & V_{ub} \\ V_{cd} & V_{cs} & V_{cb} \\ V_{td} & V_{ts} & V_{tb} \end{pmatrix} = \begin{pmatrix} 1 - \frac{\lambda^2}{2} - \frac{\lambda^4}{8} & \lambda & A\lambda^3(\rho - i\eta) \\ \lambda(-1 + A^2\frac{\lambda^4}{2}(1 - 2(\rho + i\eta))) & 1 - \frac{\lambda^2}{2} - \frac{\lambda^4}{8}(1 + 4A^2) & A\lambda^2 \\ A\lambda^3(1 - (\rho + i\eta)(1 - \frac{\lambda^2}{2})) & A\lambda^2(-1 + \frac{\lambda^2}{2}(1 - 2(\rho + i\eta))) & 1 - A^2\frac{\lambda^4}{2} \end{pmatrix}, \tag{2.2}$$

and to multiply it by the mixing matrices of the first, the second, and the third generation with the fourth generation, R_{14}, R_{24}, R_{34}, respectively, in the following way [19]:

$$V_{\mathrm{CKM4}} = R_{34} \cdot R_{24} \cdot R_{14} \cdot V_{\mathrm{CKM3}}, \tag{2.3}$$

where

$$R_{34} = \begin{pmatrix} 1 & 0 & 0 & 0 \\ 0 & 1 & 0 & 0 \\ 0 & 0 & c_u & s_u \\ 0 & 0 & -s_u & c_u \end{pmatrix}, \tag{2.4}$$

$$R_{24} = \begin{pmatrix} 1 & 0 & 0 & 0 \\ 0 & c_v & 0 & s_v e^{-i\phi_2} \\ 0 & 0 & 1 & 0 \\ 0 & -s_v e^{i\phi_2} & 0 & c_v \end{pmatrix}, \tag{2.5}$$

$$R_{14} = \begin{pmatrix} c_w & 0 & 0 & s_w e^{-i\phi_3} \\ 0 & 1 & 0 & 0 \\ 0 & 0 & 1 & 0 \\ -s_w e^{i\phi_3} & 0 & 0 & c_w \end{pmatrix}. \tag{2.6}$$

The values for the parameters λ, A, ρ, and η are taken to be in the range given by the global fit in SM3 [20]. The fourth generation parameters, $c_{u,v,w} \equiv \cos\theta_{u,v,w}$ and $s_{u,v,w} \equiv \sin\theta_{u,v,w}$, and the two new phases $\phi_{2,3}$ ($s_{\phi_2,\phi_3} \equiv \sin\phi_{2,3}$), are the new parameters which need to be fitted. The label ϕ_1 is reserved for the standard CKM3 phase appearing in (2.2). In this parametrization, all matrix elements will now depend on the new parameters; for example, the matrix element V_{ud} will have the form

$$V_{ud} = c_w\left(1 - \frac{\lambda^2}{2} - \frac{\lambda^4}{8}\right) - e^{i\phi_3}s_w(\lambda s_v e^{-i\phi_2} + A\lambda^3(\rho - i\eta)s_u c_v).$$

In order to estimate CPV phenomena with the 4th generation quarks, first we have to determine elements of the new 4×4 quark mixing matrix V_{CKM4}, (2.3), which essentially means to do a fitting of the 4th generation parameters

$$m_{b'}, m_{t'}, s_u, s_v, s_w, s_{\phi_2}, s_{\phi_3}. \tag{2.7}$$

We shall perform the fit of these parameters by analyzing $K^0 - \bar{K}^0$, $D^0 - \bar{D}^0$, and $B^0_{d,s} - \bar{B}^0_{d,s}$ mixings, and estimating the decays $K^+ \to \pi^+ \nu\bar{\nu}$ and $B \to X_s \gamma$. The fit to the new measurement of $\sin 2\beta_{\psi K}$ is added too. Moreover, in this analysis we are following strict requirement of the unitarity condition of the new matrix (2.3) at the expense of slight unitarity breaking of the CKM3 matrix. This, together with the independently measured CKM3 matrix elements [20], will give us additional constraints on the parameters of the $V_{4\times4}$ quark mixing matrix (2.1), (2.2), (2.3), (2.4), (2.5), and (2.6).

A. Definition of our fitting procedure

The fit is performed by the CERN Fortran code called MINUIT [21]. It minimizes the multiparameter function which is defined as a sum of various χ^2's between the fitted expression and the data:

$$\chi^2(\alpha) = \sum_i \frac{(\mathrm{th}(\alpha)_i - \exp_i)^2}{(\Delta \mathrm{th}_i)^2 + (\Delta \exp_i^2)}, \tag{2.8}$$

where $\mathrm{th}(\alpha)_i$ defines the 4th generation model parameter dependent predictions of a given constraint i, and exp represents the measured values. $\Delta \mathrm{th}_i$ is the uncertainty of prediction th_i and $\Delta \exp_i$ is the uncertainty of the individual measurement $\exp_i$. α is the vector of free parameters being fitted, in our case $\alpha = (s_u, s_v, s_w, s_{\phi_2}, s_{\phi_3})$. The χ^2 will in addition depend on the masses of the b' and t' quarks. The fit is performed by varying $m_{b'}$ and $m_{t'}$ in such a way that the constraint from the electroweak precision measurements is fulfilled, assuming $m_H = 115$ GeV (1.1):

$$m_{b'} = m_{t'} - 55 \text{ GeV}. \tag{2.9}$$

Much larger mass splitting would require more tuning in the canceling contributions to the EW T parameter.

A remark is in order: due to the complexity of the expressions, the uncertainties of the theoretical predictions are not taken into the fit.

B. Fitting different measured processes in the model with four generations

1. Check of the unitarity of the CKM3 matrix in SM3

First, we use the unitarity bound on the CKM3 parameters coming from the independent measurements. These are

$$\begin{aligned}
|V_{ud}|^2 + |V_{us}|^2 + |V_{ub}|^2 &= 0.9999 \pm 0.0011 \quad \text{(1st row)},\\
|V_{cd}|^2 + |V_{cs}|^2 + |V_{cb}|^2 &= 1.136 \pm 0.125 \quad \text{(2nd row)},\\
|V_{ud}|^2 + |V_{cd}|^2 + |V_{td}|^2 &= 1.002 \pm 0.005 \quad \text{(1st column)},\\
|V_{us}|^2 + |V_{cs}|^2 + |V_{ts}|^2 &= 1.134 \pm 0.125 \quad \text{(2nd column)}.
\end{aligned} \tag{2.10}$$

Also, the six CKM3 matrix elements are measured independently,

$$\begin{aligned}
|V_{ud}| &= 0.974\,18 \pm 0.000\,27,\\
|V_{us}| &= 0.2255 \pm 0.0019,\\
|V_{cd}| &= 0.230 \pm 0.011,\\
|V_{cs}| &= 1.04 \pm 0.06,\\
|V_{cb}| &= (41.2 \pm 1.1) \times 10^{-3},\\
|V_{ub}| &= (3.93 \pm 0.36) \times 10^{-3},
\end{aligned} \tag{2.11}$$

which give us additional six constraints on the unknown parameters.

2. $K^0 - \bar{K}^0$ mixing

We modify expressions for the ΔM_K, ϵ_K, and ϵ'/ϵ ratio in the model with the fourth generation in order to limit the elements $V_{t'd}$ and $V_{t's}$. The experimental values are

$$\Delta M_K = (3.483 \pm 0.006) \times 10^{-15}, \tag{2.12}$$

$$\epsilon_K \equiv |\epsilon| = (2.229 \pm 0.012) \times 10^{-3}, \tag{2.13}$$

$$\mathrm{Re}\,(\epsilon'/\epsilon) = (1.63 \pm 0.26) \times 10^{-3}. \tag{2.14}$$

3. $D^0 - \bar{D}^0$ mixing

An expression for the x_D is used in order to determine $V_{cb'}$ and $V_{ub'}$. From the experiment we have

$$x_D = 0.776 \pm 0.008. \tag{2.15}$$

4. $B^0_{d,s} - \bar{B}^0_{d,s}$ mixings

We need the x_{B_d} and x_{B_s} mixing parameters in order to bound $V_{t'd}$, $V_{t'b}$, and $V_{t's}$, $V_{t'b}$, respectively. The measured values are

$$x_{B_d} = 0.776 \pm 0.008, \tag{2.16}$$

$$x_{B_s} = 26.1 \pm 0.5. \tag{2.17}$$

5. $K^+ \to \pi^+ \nu\bar{\nu}$ process

From the branching ratio for $K^+ \to \pi^+ \nu\bar{\nu}$ we confine $V_{t'd}$ and $V_{t's}$. Recent experiments give

$$\mathrm{BR}\,(K^+ \to \pi^+ \nu \bar{\nu}) = (1.5 \pm 1.3) \times 10^{-10}. \tag{2.18}$$

6. $B \to X_s \gamma$ process

To find $V_{t'b}$ we also make use of the branching ratio for $B \to X_s \gamma$ and employ

$$\mathrm{BR}\,(B \to X_s \gamma) = (3.55 \pm 0.26) \times 10^{-4}. \tag{2.19}$$

7. $\sin 2\beta$ from $B \to J/\psi K$

In the SM3, the best measurement of the $\sin 2\beta$ comes from $B \to J/\psi K$ decay, giving

$$\beta \equiv \arg\left(-\frac{V_{cb}^* V_{cd}}{V_{tb}^* V_{td}}\right). \tag{2.20}$$

In the model with the fourth generation, the $\sin 2\beta$ can get modified with a new phase, i.e., $\sin 2\beta \to \sin(2\beta - 2\theta)$. So, we need to manipulate the expression for θ in order to determine $V_{t'b}$ and $V_{t'd}$ from the experimental data,

$$\sin 2\beta = 0.681 \pm 0.025. \tag{2.21}$$

It is important to note that in all the above processes the mass $m_{t'}$ appears explicitly in the fit, except for $D^0 - \bar{D}^0$ mixing, which depends on the $m_{b'}$ mass (2.15).

The analytic formulas for the processes are taken from various papers: for kaon mixing and decays from [22]; for $D^0 - \bar{D}^0$ mixing from [23]; for $B^0_{d,s} - \bar{B}^0_{d,s}$ mixings from [24]; for $B \to X_s \gamma$ from [25].

Various loop-induced processes depend on different Inami-Lim functions [26]. The inclusion of the 4th generation quarks in the loops brings additional Inami-Lim functions depending now on $m_{t',b'}/M_W$ and the products of the new CKM4 matrix elements $\lambda_{t'}^{bd}$, $\lambda_{t'}^{bs}$, $\lambda_{t'}^{sd}$ (and similarly for b'), where

$$\lambda_k^{lm} = V_{kl}^* V_{km}; \tag{2.22}$$

see, for example, the analysis in [27].

All QCD lattice parameters above are taken from the averages in [28]; see also [29].

We comment here that, as was pointed out in [30], there is tension between the data on B_d mixing and $\sin(2\beta)$ and the theoretical predictions for SM4, based on the lattice QCD calculations of Ref. [31]. This may signal new physics, such as SM4. Therefore, it is very important to obtain definite results for the parameters calculated in lattice QCD.

In addition, we take into account the findings of two recent studies [32,33] on the 4th generation mixing with the standard three quark families. In the first paper [32], the authors perform similar fits like ours, by using experimental constraints coming from the measured CKM3 matrix elements and FCNC processes (K, D, B_d, B_s mixings and the decay $b \to s\gamma$) and assuming the unitarity of the new $V_{4\times 4}$ matrix. As it can be seen from above, we have extended the fit adding more FCNC constraints, but our results closely follow the findings of [32], in a sense that the large mixing between 3rd and 4th generation is allowed for some range of the five-dimensional fitting space α. However, the analysis of a second paper [33] has shown that such a large mixing between third and the fourth generation, larger than the Cabibbo mixing of the first two families, is excluded by the electroweak precision data. Therefore, in addition, we apply the EW precision data constraint from [33], which implies that the maximum of $\sin\theta_{34} = \sin\theta_u$ must be in the following range:

$$\max(\sin\theta_u) = \begin{cases} 0.35 \pm 0.001 & \text{for } m_{t'} = 300\ \text{GeV} \\ 0.11 \pm 0.10 & \text{for } m_{t'} = 1000\ \text{GeV} \end{cases} \tag{2.23}$$

(for other values and for more explanations, see Table 3 in [33]). Here, the lower bound for large $m_{t'}$ masses is enlarged, due to the unreliable perturbation theory applied for the EW fits at such large energies (see discussion in [33]).

Applying all the constraints discussed above, we obtain the results presented in the next subsection.

C. Results of the fitting procedure

Here are the results for the fitted values of the vector $\alpha = (s_u, s_v, s_w, s_{\phi_2}, s_{\phi_3})$ depending on the 4th generation quark masses. Since we have just one place where the $m_{b'}$ mass enters, II B 3 above, the quark mass dependence comes mainly from the $m_{t'}$.

The experimental constraints on the $m_{t'}$ and $m_{b'}$ masses are [20,34]

$$m_{b'} > (46\text{–}199)\ \text{GeV}, \tag{2.24}$$

$$m_{t'} > 256\ \text{GeV}. \tag{2.25}$$

Therefore, we scan the $m_{t'}$ in the range of

$$300 < m_{t'} < 1000\ \text{GeV}, \tag{2.26}$$

and take care about the EW precision data limit on $m_{b'}$ and $m_{t'}$ mass difference, Eq. (2.9).

It is important to note that in models with the light Higgs, there is a unitary bound on the masses of the fourth generation quarks which amounts to $m_{b',t'} \leq 550$ GeV. If the Higgs boson is heavy ($m_H \geq 500$ GeV), the above perturbative limit does not hold, and the masses of the fourth family can be larger [2,35].

The quality of the fit is given by the minimal χ^2/d.o.f, where d.o.f (degrees of freedom) is the number of the constraints minus the number of the fitted parameters. The best fit is when $\chi^2_{\min}/\text{d.o.f} \approx 1$. For the numbers given below, d.o.f = 13.

The following results of the fitting procedure are of special importance:

(i) $m_{t'} \sim [300\text{–}600]$ GeV region is preferred by the χ^2 scan, i.e. $\chi^2_{\min}/\text{d.o.f} \approx 1$. The larger $m_{t'}$ masses do not produce a good fit, as one can see from Table I.

TABLE I. Results of our fit on the mixing between the third and the fourth generation obtained including the EW constraints from [33].

$m_{t'}$ (GeV)	$\lvert\sin\theta_u\rvert$	$\chi^2_{\rm min}$/d.o.f
300	0.25 ± 0.04	0.85
350	0.13 ± 0.03	0.98
400	0.10 ± 0.02	0.84
450	0.10 ± 0.04	0.79
500	0.10 ± 0.04	0.80
600	0.11 ± 0.03	0.93
700	0.11 ± 0.02	1.17
800	0.11 ± 0.02	1.45
900	0.11 ± 0.02	1.76
1000	0.11 ± 0.02	2.07

(ii) The best fits with $\chi^2_{\rm min}$/d.o.f ≈ 1 for $m_{t'} >$ 600 GeV give too large $s_u = \sin\theta_u$ mixing angle which is excluded by the EW precision data. On the other hand, the allowed values for s_u are obtained with the bad fit, with $\chi^2_{\rm min}$/d.o.f. > 1; see Table I.

(iii) In addition, we test the predictions for all quantities entering the fit using the new fitted parameters, in a way that we look for the "pull" [= (data central value − predicted value)/(data error)] of the data. So, although the fit for $m_{t'} = 700$ GeV has $\chi^2_{\rm min}$/d.o.f slightly larger than 1, we have decided to keep this fit, since the predictions with this mass of $m_{t'}$ nicely match with the data.

Having in mind all the facts above, we conclude that our best fits are obtained for $300 \le m_{t'} \le 700$, with the fitted parameters given in Table II, while the selected $V_{\rm CKM}$ matrix elements are presented in Table III.

The final results at 95% confidence level of the complete 4×4 fitted matrices are given below:

$$V_{\rm CKM4}(m_{t'} = 300\ {\rm GeV}) = \begin{pmatrix} 0.9742 & 0.2257 & 0.0035e^{-68.9^\circ i} & 0.0018e^{-12.4^\circ i} \\ -0.2255 & 0.9732 & 0.0414 & 0.0102e^{29.8^\circ i} \\ 0.0086e^{-24.1^\circ i} & -0.0416e^{0.7^\circ i} & 0.9649 & 0.2589 \\ -0.0019e^{18.9^\circ i} & 0.0052e^{69.3^\circ i} & -0.2591 & 0.9658 \end{pmatrix}, \tag{2.27}$$

$$V_{\rm CKM4}(m_{t'} = 400\ {\rm GeV}) = \begin{pmatrix} 0.9740 & 0.2256 & 0.0036e^{-68.9^\circ i} & 0.0164e^{-87.4^\circ i} \\ -0.2259 & 0.9728 & 0.0414 & 0.0290e^{-76.1^\circ i} \\ 0.0092e^{-27.7^\circ i} & -0.0414 & 0.9932 & 0.1079 \\ -0.0091e^{89.9^\circ i} & 0.0310e^{-94.6^\circ i} & -0.1082 & 0.9935 \end{pmatrix}, \tag{2.28}$$

$$V_{\rm CKM4}(m_{t'} = 500\ {\rm GeV}) = \begin{pmatrix} 0.9740 & 0.2256 & 0.0035e^{-68.9^\circ i} & 0.0160e^{-81.1^\circ i} \\ -0.2259 & 0.9726 & 0.0414 & 0.0329e^{-71.8^\circ i} \\ 0.0083e^{-27.1^\circ i} & -0.0416e^{6.0^\circ i} & 0.9934 & 0.1059 \\ -0.0080e^{83.2^\circ i} & 0.0344e^{-100.4^\circ i} & -0.1062e^{0.7^\circ i} & 0.9937 \end{pmatrix}, \tag{2.29}$$

$$V_{\rm CKM4}(m_{t'} = 600\ {\rm GeV}) = \begin{pmatrix} 0.9741 & 0.2256 & 0.0035e^{-68.9^\circ i} & 0.0140e^{-75.4^\circ i} \\ -0.2258 & 0.9726 & 0.0414 & 0.0339e^{-66.0^\circ i} \\ 0.0089e^{-26.2^\circ i} & -0.0423e^{6.3^\circ i} & 0.9924 & 0.1149 \\ -0.0058e^{77.9^\circ i} & 0.0343e^{-105.9^\circ i} & -0.1155e^{0.7^\circ i} & 0.9926 \end{pmatrix}, \tag{2.30}$$

$$V_{\rm CKM4}(m_{t'} = 700\ {\rm GeV}) = \begin{pmatrix} 0.9741 & 0.2256 & 0.0035e^{-68.9^\circ i} & 0.0130e^{-72.9^\circ i} \\ -0.2258 & 0.9727 & 0.0414 & 0.0309e^{-62.9^\circ i} \\ 0.0088e^{-26.2^\circ i} & -0.0423e^{5.8^\circ i} & 0.9920 & 0.1179 \\ -0.0056e^{74.7^\circ i} & 0.0309e^{-108.1^\circ i} & -0.1185e^{0.6^\circ i} & 0.9924 \end{pmatrix}. \tag{2.31}$$

Note that the fitted parameters show small 4th generation mass dependence in the preferable range of $m_{t'}$, excluding the fitted 4×4 matrix at $m_{t'} = 300$ GeV, (2.27).

TABLE II. Final results for the 4th generation parameters obtained with the acceptable quality fit.

$m_{t'}$ (GeV)	300	400	500	600	700
$\sin\theta_u$	0.25 ± 0.004	0.10 ± 0.02	0.10 ± 0.004	0.11 ± 0.03	0.11 ± 0.02
$\sin\theta_v$	0.010 ± 0.003	0.029 ± 0.001	0.034 ± 0.001	0.033 ± 0.008	0.031 ± 0.005
$\sin\theta_w$	0.002 ± 0.001	0.016 ± 0.002	0.015 ± 0.001	0.014 ± 0.001	0.012 ± 0.001
$\sin\phi_2$	-0.4 ± 0.4	0.97 ± 0.01	0.947 ± 0.002	0.91 ± 0.02	0.89 ± 0.04
$\sin\phi_3$	0.2 ± 0.3	0.99 ± 0.02	0.987 ± 0.001	0.96 ± 0.03	0.95 ± 0.03

TABLE III. Predictions for the selected $V_{\rm CKM}$ matrix elements using the best fit from Table II.

$m_{t'}$ (GeV)	300	400	500	600	700
$\lvert V_{tb}\rvert$	0.964 ± 0.010	0.993 ± 0.003	0.993 ± 0.001	0.992 ± 0.003	0.992 ± 0.003
$\lvert V_{tb'}\rvert$	0.258 ± 0.037	0.107 ± 0.022	0.106 ± 0.004	0.115 ± 0.025	0.118 ± 0.028
$\lvert V_{t'b}\rvert$	0.259 ± 0.037	0.108 ± 0.022	0.106 ± 0.004	0.115 ± 0.025	0.118 ± 0.028
$\lvert V_{t'b'}\rvert$	0.965 ± 0.010	0.993 ± 0.003	0.994 ± 0.001	0.992 ± 0.003	0.992 ± 0.003
$\lvert V_{t'd}\rvert$	0.002 ± 0.001	0.009 ± 0.002	0.008 ± 0.001	0.006 ± 0.001	0.006 ± 0.001
$\lvert V_{t's}\rvert$	0.005 ± 0.005	0.031 ± 0.001	0.034 ± 0.007	0.034 ± 0.009	0.031 ± 0.005
$\lvert V_{ub'}\rvert$	0.002 ± 0.001	0.016 ± 0.002	0.016 ± 0.004	0.014 ± 0.001	0.013 ± 0.002
$\lvert V_{cb'}\rvert$	0.010 ± 0.003	0.030 ± 0.001	0.033 ± 0.002	0.034 ± 0.009	0.031 ± 0.005

From the above matrices we can see that the fit exhibits constraint $|V_{tb}| > 0.96$, which is much stronger than the limit $|V_{tb}| > 0.74$ following from the single top-quark production cross section measurement [20].

Comparing our results with those existing in the literature [32,36,37], we can deduce that our fit, under the conditions specified in Sec. II B, excludes large mixing between 4th and the first three generations. Our matrix elements $|V_{ub'}|$, $|V_{cb'}|$, $|V_{tb'}|$ from Table III are significantly smaller (up to 6 times for $|V_{tb'}|$) with respect to the same elements obtained by the conservative bound in [32] and in [38]. This is a direct consequence of the applied EW constraint on $\sin\theta_u$, (2.23), since otherwise, as already mentioned at the end of Sec. II B, the somewhat larger mixing between the third and the fourth generation, relative to the bound from Eq. (2.23), is obtained. In [27], the mixing is bounded to $\sin\theta_{34} \le 0.14$.

Considering phases of CKM4, in our approach they are strongly depending on the $m_{t'}$ mass, oscillating widely, as they do in [32]. In [27], as well as in [32,38], the fits are performed under the assumption that the phases are free and run between 0 and 2π. However, in our global and unique fit, which generates matrices (2.27), (2.28), (2.29), (2.30), and (2.31), the phases are also subject to the fitting procedure. Therefore, the complex interplay between all fitting parameters can significantly influence the final allowed parameter values of the matrix elements.

Although the standard CKM3 matrix elements, as a part of $V_{\rm CKM4}$, were fitted, in our fit their values (2.27), (2.28), (2.29), (2.30), and (2.31) do not contradict the global CKM3 fit from [20]. This is especially true for the less constrained elements like V_{td} and V_{ts}.

The obtained fourth generation parameter values (2.27), (2.28), (2.29), (2.30), and (2.31) will be used in the calculation of the rare decay branching ratios and CP partial rate asymmetry in the next sections.

III. RARE PROCESSES INVOLVING THE FOURTH GENERATION

We analyze FCNC decay processes of the fourth generation quarks, in particular, of $t' \to (c, t)X$ and $b' \to (s, b)X$ with $(X = H, Z, \gamma, g)$, arising from the generic one-loop diagrams given in Fig. 1. We also study the influence of the 4th generation FCNC model to the ordinary top-quark rare decays: $t \to cX$.

The rare FCNC processes of the above type have been extensively studied in the context of various extensions of SM. We base our study on the explicit analytical expressions on $Q \to q(Z, \gamma, g)$ given in [39], with $Q = (t, t', b')$ and $q = (c, (t, c), (b, s))$, respectively. Checks for $Q \to q(\gamma, g)$ decays are performed using expressions from [40]. The $Q \to qH$ decays were considered in [41].

To obtain the branching ratios, the decay amplitudes will be normalized to the widths of the decaying quarks. For t-quark decays we have

$$\mathrm{BR}\,(t \to cX) = \frac{\Gamma(t \to cX)}{\Gamma(t \to bW)}, \tag{3.1}$$

while for t' and b' decays, we will also take into account the CKM4-suppressed tree level decays. Therefore,

$$\mathrm{BR}\,(t' \to (c, t)X) = \frac{\Gamma(t' \to (c, t)X)}{\Gamma(t' \to bW) + \Gamma(t' \to sW)}, \tag{3.2}$$

$$\mathrm{BR}\,(b' \to (s, b)X) = \frac{\Gamma(b' \to (s, b)X)}{\Gamma(b' \to tW^{(*)}) + \Gamma(b' \to cW)}, \tag{3.3}$$

where $b' \to tW^*$ is effective for $m_{b'} \le 255$ GeV. The tree

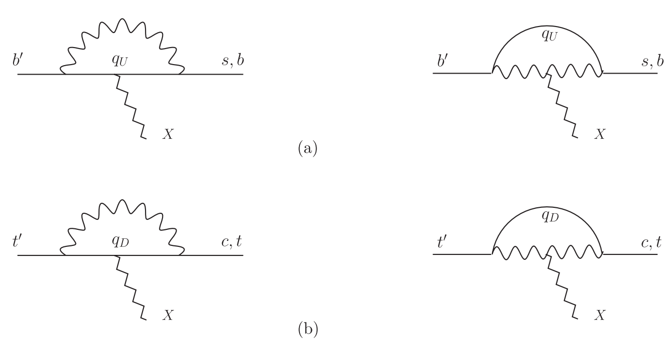

FIG. 1. Generic diagrams for FCNC decays of the 4th generation quarks. X denotes possible decays to $X = H, Z, \gamma, g$ and quarks running in the loops are $q_U = \{u, c, t, t'\}$ and $q_D = \{d, s, b, b'\}$. (a) b' decays and (b) t' decays.

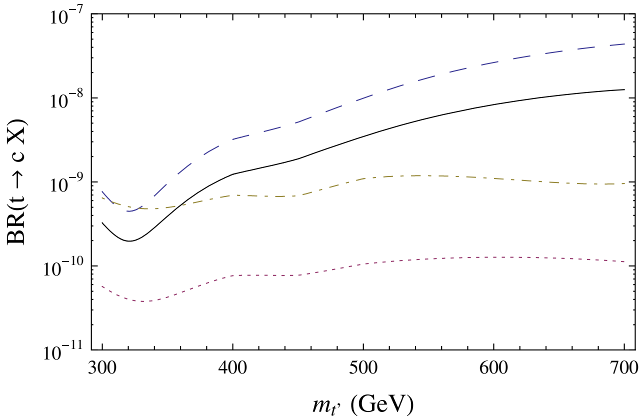

FIG. 2 (color online). Branching ratios for rare top decays in the model with 4th generation as a function of $m_{t'}$, for b' of the mass $m_{b'} = m_{t'} - 55$ GeV running in the loops. X denotes possible decays to $X = H$ (dashed line), Z (solid line), γ (dotted line), g (dash-dotted line).

level decays are given by

$$\Gamma(Q \to qW) = \frac{G_F M_W^3 x_Q^3}{8\pi\sqrt{2}} |V_{Qq}|^2 \sqrt{\lambda(1, (1/x_Q)^2, (x_q/x_Q)^2)} \times ((1 - x_q^2/x_Q^2)^2 + 1/x_Q^2(1 + x_q^2/x_Q^2) - 2/x_Q^4), \tag{3.4}$$

where $\lambda(x, y, z) = x^2 + y^2 + z^2 - 2xy - 2xy - 2yz$ and $x_i^2 = m_i^2/M_W^2$. The masses running in the loops in Figs. 1 are taken to be current quark masses, while the external masses are considered as pole masses. Practically, this makes no numerical difference in the calculation, apart from $t \to cX$ decays with b-quark running in the loops. There we take $\bar{m}_b(m_t) = 2.74$ GeV, [40], and, with our set of parameters and $m_t = 171.2$ GeV, we obtain the following SM results:

$$\begin{aligned} \mathrm{BR}_{\mathrm{SM}}(t \to c\gamma) &= 4.4 \times 10^{-14}, \\ \mathrm{BR}_{\mathrm{SM}}(t \to cg) &= 3.8 \times 10^{-12}, \\ \mathrm{BR}_{\mathrm{SM}}(t \to cZ) &= 1.3 \times 10^{-14}, \\ \mathrm{BR}_{\mathrm{SM}}(t \to cH) &= 7.8 \times 10^{-15}, \end{aligned} \tag{3.5}$$

comparable with the estimates given in [40,42]. With the pole masses running in the loops [39], the results become an order of magnitude larger. The values from Eqs. (3.5) have to be compared with the largely enhanced BRs of $t \to cX$ for 4th generation quarks included in the loops; Fig. 2. The foreseen sensitivities for $t \to cX$ channels at Tevatron and/or LHC could be sufficient to see these enhanced rates.

Throughout the calculation, the mass of the Higgs boson is taken to be $m_H = 115$ GeV. Our fit favors fourth generation masses slightly larger than the so-called unitary bound of $\sim$600 GeV. In that case the concept of light Higgs boson and the elementary scalar Higgs field is no more appropriate, since the Goldstone boson of the electroweak symmetry breaking would couple very strongly to the heavy 4th generation quarks [2,35]. Therefore, the results for $m_{t',b'} \geq 600$ GeV have to be taken with precaution.

In the analysis we have also examined the influence of the W-boson width to the results. The inclusion of the finite width for the W boson propagating through the loops, [43], is effective only for the $t \to cX$ decays, enhancing BRs by some 10%.

Our prediction for BR($t \to cH$) given in Fig. 2, contrary to [36], always dominates over Z, γ, g modes, in the whole range of t' mass. For $t' \to (c, t)X$ (Fig. 3) and $b' \to (s, b)X$ (Fig. 4) the decay mode's general behavior is more or less the same, except that for our global fit both the gluon and the Higgs modes dominate over Z and photon modes, apart from the case given in Fig. 4(b), where H and Z dominate over g and γ modes, respectively. In [36], dominating

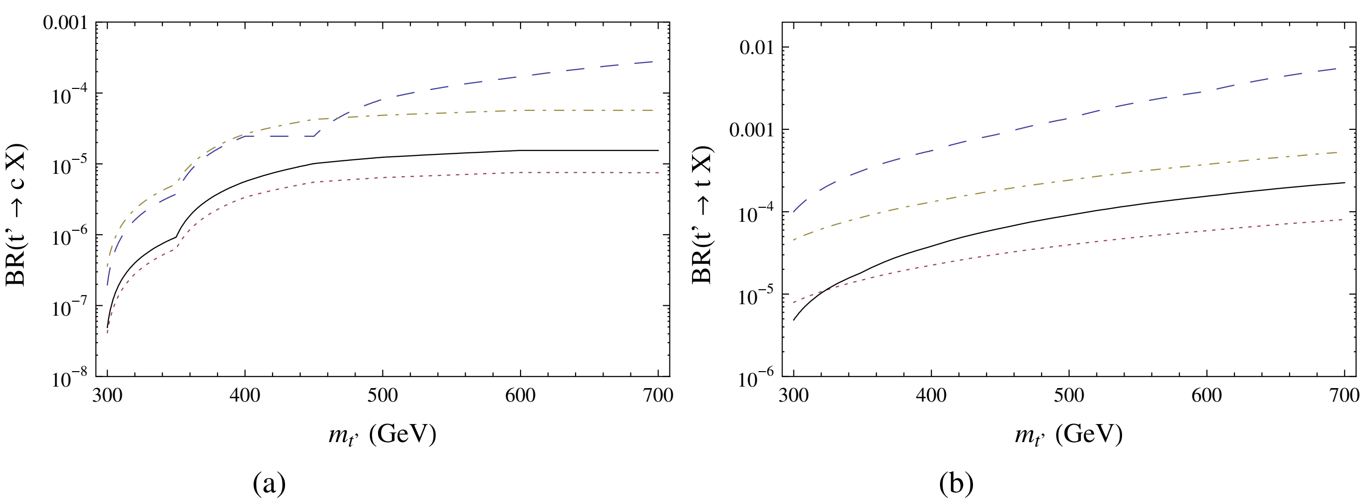

FIG. 3 (color online). Branching ratios of $t' \to (c, t)X$ as a function of $m_{t'} = m_{b'} + 55$ GeV. X denotes possible decays to $X = H$ (dashed line), Z (solid line), γ (dotted line), g (dash-dotted line). (a) BR($t' \to cX$) and (b) BR($t' \to tX$).

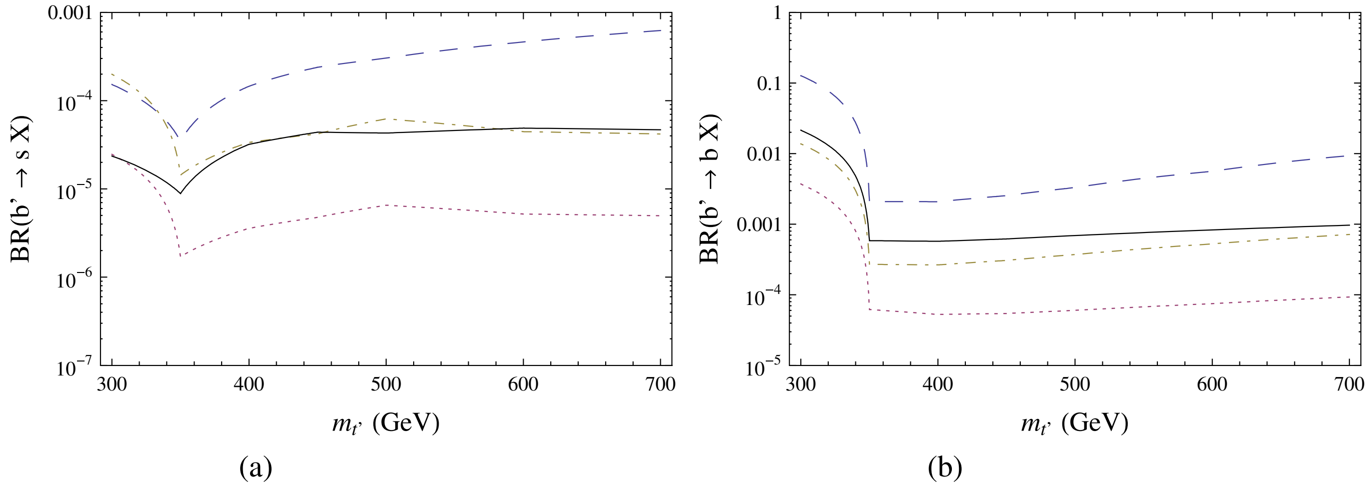

FIG. 4 (color online). Branching ratios of $b' \to (s, b)X$ as a function of $m_{t'} = m_{b'} + 55$ GeV. X denotes possible decays to $X = H$ (dashed line), Z (solid line), γ (dotted line), g (dash-dotted line). (a) BR($b' \to sX$) and (b) BR($b' \to bX$).

modes are Z and the decay into gluon, which is due to a large difference between our CKM4 parameters and the parameters used in [36].

IV. *CP* VIOLATION

The *CP* partial rate asymmetry, for decays discussed above, is defined as

$$a_{CP} = \frac{\Gamma(Q \to qX) - \Gamma(\bar{Q} \to \bar{q}\bar{X})}{\Gamma(Q \to qX) + \Gamma(\bar{Q} \to \bar{q}\bar{X})}. \tag{4.1}$$

Since the rates involve at least two amplitudes with different *CP*-conserving strong phases coming from the absorptive parts of the loops, while the *CP*-violating weak phases are provided by the phases in V_{CKM4}, we expect to find *CP* violation in FCNC decays of 4th generation quarks [44]. The inclusion of the finite W-boson width can enhance a *CP* asymmetry by enhancing the *CP*-conserving phases, but, since this happens almost equally for $\Gamma(Q \to qX)$ and $\Gamma(\bar{Q} \to \bar{q}\bar{X})$, the effect appears to be at most of 10% level. Estimated *CP* asymmetries, shown in Figs. 5–7 for FCNC rare decay modes, in general oscillate as a function of t' mass. In particular, important modes for CPV effects are $b' \to sX$ decays, as also noted recently in [37]. For $b' \to s(H, Z)$ modes we find very interesting maximal *CP* partial rate asymmetry at $m_{t'} = 300$ GeV, i.e., 94% and 62%, respectively. These large numbers occur due to the tW loop threshold at $m_{b'} \simeq 250$ GeV. Two other modes, $b' \to s(\gamma, g)$, produce maximal CPV at $m_{t'} = 350$ GeV in the amount of 47% and 41% for γ and g, respectively, and they could be important too; Fig. 7(a). Maximal *CP* partial rate asymmetry for $t \to cX$ modes occurs also at $m_{t'} = 350$ GeV for $t \to cg$, and it amounts to 18%; Fig. 5. For $t' \to (c, t)X$ and $b' \to bX$ modes a_{CP} is very small, always bellow 0.25%; Figs. 6 and 7(b).

At the end, let us discuss some general features of the *CP* violation within the model with the 4th family.

Following the analysis of Ref. [45], we calculate the strengths $|B_i|$ of *CP* violation for a fourth family in the chiral limit $m_{u,d,c} = 0$. Definitions of the relevant imaginary products in the chiral limit are [45]

$$B_1 \equiv \mathrm{Im} V_{cb} V^*_{t'b} V_{t'b'} V^*_{cb'}, \tag{4.2}$$

$$B_2 \equiv \mathrm{Im} V_{tb} V^*_{t'b} V_{t'b'} V^*_{tb'}, \tag{4.3}$$

$$B_3 \equiv \mathrm{Im} V_{cb} V^*_{tb} V_{tb'} V^*_{cb'}. \tag{4.4}$$

In [45] a rigorous upper bound on $|B_i| \leq 10^{-2}$ in the model with the 4th family was obtained. Calculating these quantities explicitly for the values of our CKM4 matrix elements (2.27), (2.28), (2.29), (2.30), and (2.31), we obtain the strengths of the *CP* violation of the order

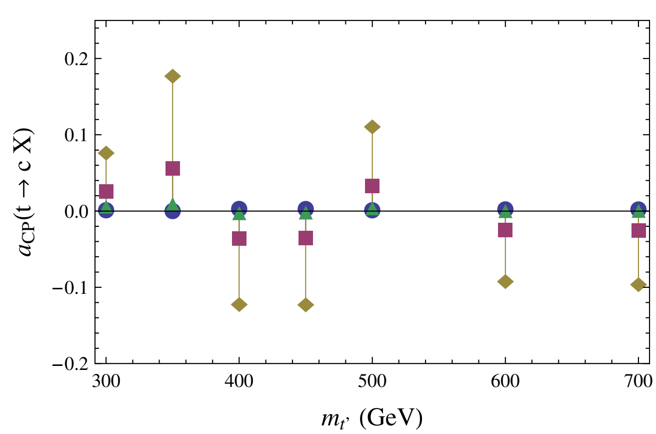

FIG. 5 (color online). Fourth generation effect on the a_{CP} of the rare top decays as a function of $m_{t'}$, for b' of the mass $m_{b'} = m_{t'} - 55$ GeV running in the loops. X denotes possible decays to $X = H$ (●), Z (▲), γ (■), g (◆).

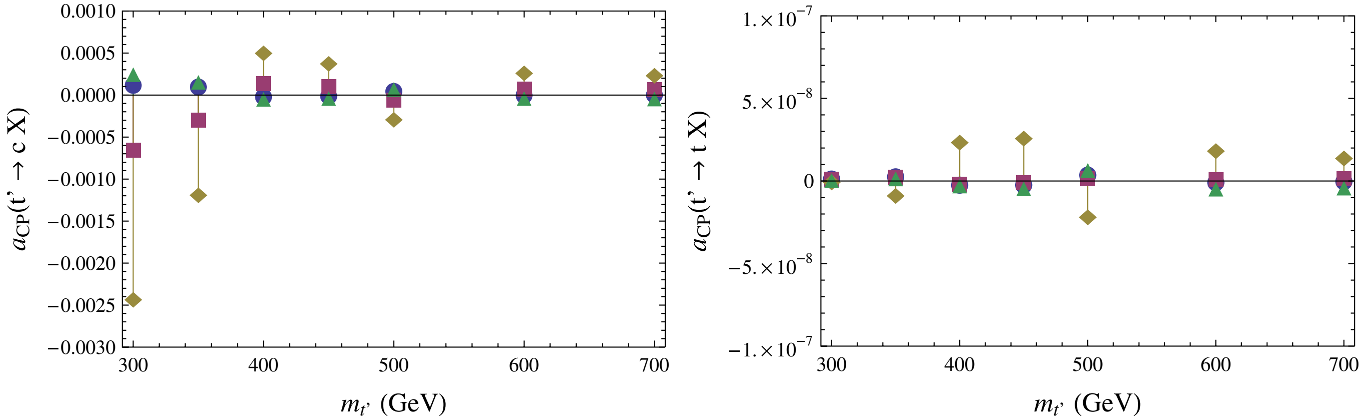

(a) $a_{CP}(t' \to cX)$ (b) $a_{CP}(t' \to tX)$

FIG. 6 (color online). *CP* asymmetries in $t' \to (c, t)X$ decays as a function of $m_{t'} = m_{b'} + 55$ GeV. X denotes possible decays to $X = H$ (●), Z (▲), γ (■), g (◆). (a) $a_{CP}(t' \to cX)$ and (b) $a_{CP}(t' \to tX)$.

$$|B_{1,2,3}| \simeq \begin{cases} 5 \times 10^{-5} & \text{for } m_{t'} = 300 \text{ GeV} \\ 10^{-4} & \text{for } m_{t'} = [400\text{–}700] \text{ GeV}. \end{cases} \quad (4.5)$$

The area of the unitary quadrangle $A_{bb'}$, with the sides $V_{ub}V^*_{ub'}$, $V_{cb}V^*_{cb'}$, $V_{tb}V^*_{tb'}$, $V_{t'b}V^*_{t'b'}$, describing CPV in the chiral limit, is

$$A_{bb'} = \frac{1}{4}\{|B_1 + B_2| + |B_1 + B_3| + |B_2| + |B_3|\}, \quad (4.6)$$

and with our fitted parameters amounts to

$$2A_{bb'} \simeq \begin{cases} 10^{-5} & \text{for } m_{t'} = 300 \text{ GeV} \\ 4 \times 10^{-4} & \text{for } m_{t'} = [400\text{–}700] \text{ GeV}. \end{cases} \quad (4.7)$$

The same values are obtained for the area of the unitary quadrangle from Eq. (1.4), defined by the unitarity relation $V_{us}V^*_{ub} + V_{cs}V^*_{cb} + V_{ts}V^*_{tb} + V_{t's}V^*_{t'b} = 0$. This has to be compared with the amount of CPV in the three-generation SM given by $|\mathrm{Im}V_{ij}V^*_{kj}V_{kj}V^*_{il}| \leq 5 \times 10^{-5}$.

We see that the measure of the CPV in the 4th generation model is only slightly larger than the amount of CPV in SM3, and this happens only for larger extra quark masses. It seems that extra quarks can give us new sources of large CPV phenomena, but, in general, cannot bring significant cumulative effect in the strength of CPV (4.7). Therefore, a huge enhancement in the Jarlskog invariant J^{bs}_{234} (1.4), in the model with the 4th family, comes predominantly from the large $m_{b'}$ and $m_{t'}$.

V. DISCUSSION AND CONCLUSIONS

In this paper we investigate the *CP*-violating decay processes involving the fourth quark generation and find large *CP* partial rate asymmetries for some decay modes. We achieve that by constructing and employing a global unique fit of the unitary CKM4 mass matrix. Our fit for certain values of the 4th generation quark mixing matrix elements for $300 \leq m_{t'} \leq 700$ GeV produces highly en-

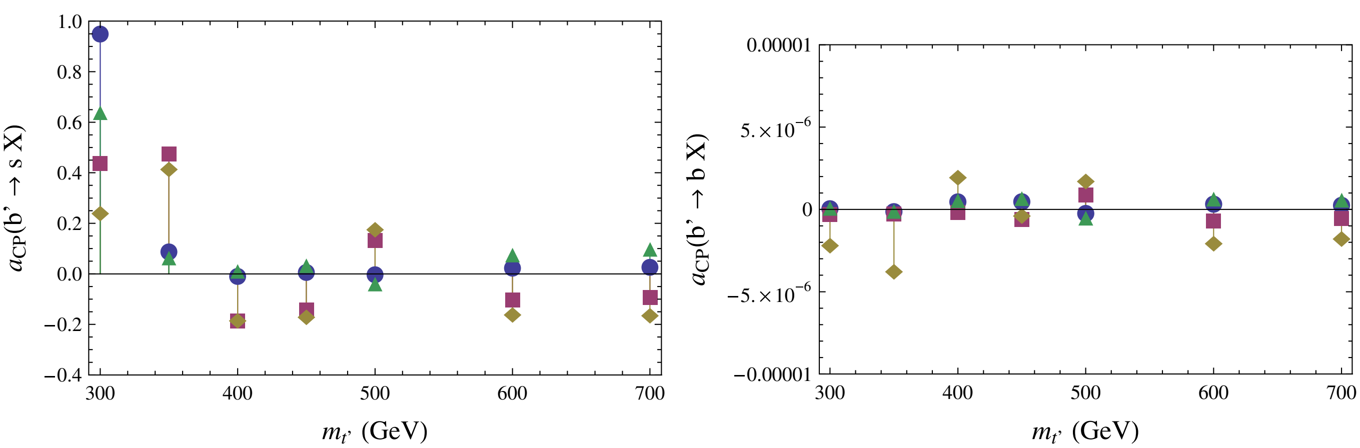

(a) (b)

FIG. 7 (color online). *CP* asymmetries in $b' \to (s, b)X$ decays as a function of $m_{t'} = m_{b'} + 55$ GeV. X denotes possible decays to $X = H$ (●), Z (▲), γ (■), g (◆). (a) $a_{CP}(b' \to sX)$ and (b) $a_{CP}(b' \to bX)$.

hanced a_{CP} for $b' \to s$ decay modes. A dominance of $a_{CP}(b' \to s(H, Z; \gamma, g)) = (95, 62; 47, 41)\%$ at $m_{t'} \simeq 300, 350$ GeV with respect to all other modes is particularly interesting.

It is important to note here that all quantities appearing in the 4th generation mixing matrix were subject to our fitting procedure, contrary to [27,32,38]. So, the phases of $V_{\rm CKM4}$ are fitted too, and the complex interplay between all fitted parameters significantly influences the final fit of the matrix elements (2.27), (2.28), (2.29), (2.30), and (2.31), and therefore the estimated CP partial rate asymmetries as well.

We have inspected FCNC decay processes of the 4th generation quarks, $b' \to sX$, $b' \to bX$, $t' \to cX$, $t' \to tX$, with $X = H, Z, \gamma, g$, and the top decays $t \to cX$ for 4th generation quarks running in the loops. The branching ratios of these rare top decays get highly enhanced due to the presence of the 4th family quarks. Considering first the CPV effects for $t \to cX$ modes, we have found $|a_{CP}(t \to cg)| \simeq 8$–$18\%$ at $m_{t'} = 300$–700 GeV; for $t \to c\gamma$ mode a_{CP} is always below 6%, while for $t \to c(H, Z)$ asymmetries are negligible; Fig. 5. The a_{CP}, as a function of t' mass between 300 and 700 GeV, oscillate for all decay modes; Figs. 5–7. As already noted, the $b' \to s(H, Z)$ modes with 95(62)% CP asymmetries at $m_{t'} = 300$ GeV dominate absolutely due to the tW loop threshold at $m_{b'} \simeq 250$ GeV. However, $a_{CP} = 47(41)\%$ for two other modes, $b' \to s(\gamma, g)$, Fig. 7(a), are more reliable as theoretical predictions and for measurements as well. Namely, the theoretical fact is that $a_{CP}(b' \to s(\gamma, g))$ receive maximal values for $m_{t'} \simeq 350$ GeV, which is shifted away from the tW loop threshold. From the experimental point of view the best decay mode, out of $b' \to s$ modes, is certainly $b' \to s\gamma$, because of the presence of a clean signal from the high energy single photon in the final state. However, the bad point is the fact that $\mathrm{BR}(b' \to s\gamma)$, at $m_{t'} = 350$ GeV, could be as small as 10^{-6}, Fig. 4(a), which is at the edge of the observable region for the LHC. On the other hand, the shift down from $m_{t'} = 350$ GeV to $m_{t'} = 300$ GeV increases $\mathrm{BR}(b' \to s\gamma)$ more than 1 order of magnitude [see Fig. 4(a)], and only slightly decreases $a_{CP}(b' \to s\gamma)$ from 47% to 42% [Fig. 7(a)]. Therefore, for $m_{b'} = 300, 350$ GeV the required number of b' quarks produced, in order to obtain a 3σ CP-violation effect, is $N_{b'} = 2.6 \times 10^6, 4.1 \times 10^7$, respectively, which is a goal attainable after a few years of operating the LHC [46] at $\mathcal{O}$(few100) fb^{-1}.

Comparing our estimate for $a_{CP}(b' \to s\gamma) = 47\%$ [see Fig. 7(a)] with very recent predictions of Ref. [37], we have found agreement up to expected differences coming from the fitting procedure and the fitted CKM4 elements (2.27), (2.28), (2.29), (2.30), and (2.31).

Discussing implications for the collider experiments we conclude that there are fair chances for the 4th generation quarks b' and t' to be observed at LHC and that their branching ratios could be measured. If LHC or future colliders discover 4th generation quarks at energies we assumed, it is highly probable that with well executed tagging large CP partial rate asymmetry could be found too.

ACKNOWLEDGMENTS

We would like to acknowledge M. Vysotsky for many stimulating comments, discussions, and careful reading of the manuscript. Comments from A. Soni are also appreciated. B. M. acknowledges the hospitality of Department of Physics, Technion, Haifa, and G. E. wishes to thank the members of the Theoretical Physics Department at the Rudjer Bošković Institute, Zagreb, for their kind hospitality. The work of B. M. and J. T. is supported by the Croatian Ministry of Science Education and Sports Projects No. 098-0982930-2864 and No. 098-0982930-2900, respectively. Work of G. E. received financial support from Technion, Haifa. The work of J. T. is also in part supported by the EU (HEPTOOLS) project under Contract No. MRTN-CT-2006-035505.

[1] P. H. Frampton, P. Q. Hung, and M. Sher, Phys. Rep. **330**, 263 (2000).
[2] B. Holdom, W. S. Hou, T. Hurth, M. L. Mangano, S. Sultansoy, and G. Unel, arXiv:0904.4698.
[3] V. A. Novikov, L. B. Okun, A. N. Rozanov, and M. I. Vysotsky, Phys. Lett. B **529**, 111 (2002); V. A. Novikov, A. N. Rozanov, and M. I. Vysotsky, arXiv:0904.4570.
[4] G. D. Kribs, T. Plehn, M. Spannowsky, and T. M. P. Tait, Phys. Rev. D **76**, 075016 (2007); H.-J. He, N. Polonsky, and S. Su, Phys. Rev. D **64**, 053004 (2001).
[5] M. E. Peskin and T. Takeuchi, Phys. Rev. D **46**, 381 (1992).
[6] P. Q. Hung, Phys. Rev. Lett. **80**, 3000 (1998).
[7] W. S. Hou, R. S. Willey, and A. Soni, Phys. Rev. Lett. **58**, 1608 (1987); **60**, 2337 (1988); G. Eilam, J. L. Hewett, and T. G. Rizzo, Phys. Lett. B **193**, 533 (1987).
[8] N. G. Deshpande and J. Trampetic, Phys. Rev. D **40**, 3773 (1989).
[9] N. G. Deshpande and J. Trampetic, Phys. Rev. D **41**, 2926 (1990).
[10] W. S. Hou, A. Soni, and H. Steger, Phys. Rev. Lett. **59**, 1521 (1987).
[11] B. Holdom, Phys. Rev. Lett. **57**, 2496 (1986); **58**, 177 (1987); W. A. Bardeen, C. T. Hill, and M. Lindner, Phys. Rev. D **41**, 1647 (1990); T. Elliott and S. F. King, Z. Phys. C **58**, 609 (1993); G. Burdman and L. Da Rold, J. High

Energy Phys. 12 (**2007**) 086.

[12] J. Alwall *et al.*, Eur. Phys. J. C **49**, 791 (2007).

[13] W. S. Hou, M. Nagashima, and A. Soddu, Phys. Rev. Lett. **95**, 141601 (2005); A. Soni, arXiv:0907.2057; A. Soni, A. K. Alok, A. Giri, R. Mohanta, and S. Nandi, arXiv:0807.1971. For another application to B physics see, i.e., K. Zeynali and V. Bashiry, Phys. Rev. D **78**, 033001 (2008).

[14] W. S. Hou, Chin. J. Phys. (Taipei) **47**, 134 (2009).

[15] C. Jarlskog, Phys. Rev. Lett. **55**, 1039 (1985).

[16] R. Fok and G. D. Kribs, Phys. Rev. D **78**, 075023 (2008).

[17] Y. Kikukawa, M. Kohda, and J. Yasuda, Prog. Theor. Phys. **122**, 401 (2009).

[18] L. Wolfenstein, Phys. Rev. Lett. **51**, 1945 (1983).

[19] F. J. Botella and L. L. Chau, Phys. Lett. B **168**, 97 (1986). For other parametrizations see, e.g., H. Harari and M. Leurer, Phys. Lett. B **181**, 123 (1986) and Ref. [10].

[20] C. Amsler *et al.* (Particle Data Group), Phys. Lett. B **667**, 1 (2008).

[21] CERN MINUIT—physics analysis tool for function minimization, http://lcgapp.cern.ch/project/cls/work-packages/mathlibs/minuit/home.html.

[22] T. Hattori, T. Hasuike, and S. Wakaizumi, Phys. Rev. D **60**, 113008 (1999); A. J. Buras, arXiv:hep-ph/0101336; A. J. Buras and M. Jamin, J. High Energy Phys. 01 (2004) 048; J. F. Donoghue, E. Golowich, B. R. Holstein, and J. Trampetic, Phys. Lett. B **179**, 361 (1986); **188**, 511 (1987).

[23] E. Golowich, J. Hewett, S. Pakvasa, and A. A. Petrov, Phys. Rev. D **76**, 095009 (2007); J. F. Donoghue, E. Golowich, B. R. Holstein, and J. Trampetic, Phys. Rev. D **33**, 179 (1986); G. Burdman, E. Golowich, J. L. Hewett, and S. Pakvasa, Phys. Rev. D **66**, 014009 (2002).

[24] A. J. Buras, M. Jamin, and P. H. Weisz, Nucl. Phys. **B347**, 491 (1990); A. Lenz and U. Nierste, J. High Energy Phys. 06 (2007) 072; M. Beneke, G. Buchalla, C. Greub, A. Lenz, and U. Nierste, Phys. Lett. B **459**, 631 (1999); M. Beneke, G. Buchalla, A. Lenz, and U. Nierste, Phys. Lett. B **576**, 173 (2003); M. Ciuchini, E. Franco, V. Lubicz, F. Mescia, and C. Tarantino, J. High Energy Phys. 08 (2003) 031.

[25] C. Greub and T. Hurth, Phys. Rev. D **56**, 2934 (1997); A. L. Kagan and M. Neubert, Eur. Phys. J. C **7**, 5 (1999); A. J. Buras, arXiv:hep-ph/9806471.

[26] T. Inami and C. S. Lim, Prog. Theor. Phys. **65**, 297 (1981); **65**, 1772 (1981).

[27] T. Yanir, J. High Energy Phys. 06 (2002) 044.

[28] V. Lubicz and C. Tarantino, Nuovo Cimento Soc. Ital. Fis. B **123**, 674 (2008).

[29] A. J. Buras and D. Guadagnoli, Phys. Rev. D **79**, 053010 (2009); M. Blanke, A. J. Buras, B. Duling, S. Recksiegel, and C. Tarantino, arXiv:0906.5454.

[30] E. Lunghi and A. Soni, Phys. Lett. B **666**, 162 (2008).

[31] D. J. Antonio *et al.* (RBC Collaboration and UKQCD Collaboration), Phys. Rev. Lett. **100**, 032001 (2008).

[32] M. Bobrowski, A. Lenz, J. Riedl, and J. Rohrwild, Phys. Rev. D **79**, 113006 (2009).

[33] M. S. Chanowitz, Phys. Rev. D **79**, 113008 (2009).

[34] T. Aaltonen *et al.* (CDF Collaboration), Phys. Rev. D **76**, 072006 (2007); Phys. Rev. Lett. **100**, 161803 (2008); P. Q. Hung and M. Sher, Phys. Rev. D **77**, 037302 (2008).

[35] B. Holdom, J. High Energy Phys. 08 (2006) 076.

[36] A. Arhrib and W. S. Hou, J. High Energy Phys. 07 (2006) 009.

[37] A. Arhrib and W. S. Hou, Phys. Rev. D **80**, 076005 (2009).

[38] J. A. Herrera, R. H. Benavides, and W. A. Ponce, Phys. Rev. D **78**, 073008 (2008).

[39] G. Eilam, J. L. Hewett, and A. Soni, Phys. Rev. D **44**, 1473 (1991); **59**, 039901 (1998); G. Eilam, M. Frank, and I. Turan, Phys. Rev. D **73**, 053011 (2006).

[40] J. A. Aguilar-Saavedra and B. M. Nobre, Phys. Lett. B **553**, 251 (2003).

[41] B. Haeri, A. Soni, and G. Eilam, Phys. Rev. Lett. **62**, 719 (1989); G. Eilam, B. Haeri, and A. Soni, Phys. Rev. D **41**, 875 (1990); B. Mele, S. Petrarca, and A. Soddu, Phys. Lett. B **435**, 401 (1998); W. S. Hou and R. G. Stuart, Phys. Lett. B **233**, 485 (1989); W. S. Hou and R. G. Stuart, Phys. Rev. D **43**, 3669 (1991).

[42] J. A. Aguilar-Saavedra, Acta Phys. Pol. B **35**, 2695 (2004).

[43] G. Eilam, J. L. Hewett, and A. Soni, Phys. Rev. Lett. **67**, 1979 (1991); J. M. Soares, Phys. Rev. Lett. **68**, 2102 (1992); G. Eilam, J. L. Hewett, and A. Soni, Phys. Rev. Lett. **68**, 2103 (1992).

[44] D. Atwood, S. Bar-Shalom, G. Eilam, and A. Soni, Phys. Rep. **347**, 1 (2001).

[45] F. del Aguila, J. A. Aguilar-Saavedra, and G. C. Branco, Nucl. Phys. **B510**, 39 (1998).

[46] CMS Physics Technical Design Report No. CERN/LHCC 2006-001, Vol. 1; M. Pieri *et al.*, CMS Note 2006/112.